

Master Thesis

Development of a Control System to Improve the Stability of the FLUTE Electron Gun

Marvin-Dennis Noll

Supervisors: Prof. Dr.-Ing. John Jelonnek (IHM)
Prof. Dr. Anke-Susanne Müller (IBPT)
Advisor: Dr. Nigel Smale (IBPT)

Period: 15.11.2020 – 07.07.2021

Karlsruhe, 07.07.2021



Institute for Beam Physics and Technology
Hermann-von-Helmholtz-Platz 1
Campus North, Building 348
76344 Eggenstein-Leopoldshafen



Institute for Pulsed Power and Microwave Technology
Hermann-von-Helmholtz-Platz 1
Campus North, Building 421
76344 Eggenstein-Leopoldshafen

Declaration

I hereby declare that I wrote my master thesis on my own and that I have followed the regulations relating to good scientific practice of the Karlsruhe Institute of Technology (KIT) in its latest form. I did not use any unacknowledged sources or means, and I marked all references I used literally or by content.

Karlsruhe, 16.07.2021

Marvin-Dennis Noll

Abstract

The compact linear accelerator *Ferninfrarot Linac- und Test-Experiment* (FLUTE) is currently under commission at Karlsruhe Institute of Technology (KIT). Its main purposes are to serve as a technology platform for accelerator research and the generation of strong and ultra short terahertz (THz) pulses.

The electron gun and the Linear Accelerator (LINAC) are powered by a klystron. It is fed by a pulse forming network, which is driven by a high voltage source connected to mains power. For stable energies of the generated THz pulses, the electron energies have to be stable. To ensure stable energies of the emitted electron bunches, several parameters of the gun, such as temperature and the Radio Frequency (RF) power supply from the klystron, have to stay inside tight tolerance bands.

In this work, instead of passively optimizing the stability of system components, such as the water coolers or power supplies, an active approach with a closed feed-back loop is evaluated. By means of a control system, the amplitude of the low power RF input signal of the klystron is manipulated to mitigate the effects of noise and drifts on the electron energy. As there is currently no sensor to measure the electron energies of all the electron bunches, the RF power in the first gun cavity is used instead as an estimator for the electron energy stability.

As part of the development process, first the stability issue is analyzed and metrics for quantifying the stability are defined. Then, an appropriate solution, a linear, discrete time control system, is proposed. In order to implement it, all the necessary building blocks of such a control system are treated in detail. First the necessary sensors and actuators are selected. Then the controller and the measurement filter are designed. To verify the designed system, first an offline simulation on a computer is performed which shows qualitatively a satisfactory disturbance rejection with a measured disturbance signal from FLUTE.

Then the control system is implemented as an algorithm with a fixed-interval control loop using the Python programming language. A graphical user interface, written in Qml, provides the user with plots and status information and allows the fine-tuning of the controller.

The following experiments at FLUTE show results in accordance to the simulation. That is, the stability, when defined as the relative standard deviation, is improved greatly by about a factor of 25.

Finally ways to refine the control system are regarded. First by using disturbance feed-forward of the change in waster temperature, the control system is made more robust and achieves the same results. Second the usage of a Faraday cup, which measures total electron charge provides a potentially better representation of the electron energies, however as the electron beam is lost in the cup, its usages are limited.

Contents

1	The Stability of FLUTE the Electron Gun and Proposed Stabilizing Solution	1
1.1	The Electron Gun	2
1.2	Relation between RF power and Electron Energy	3
1.3	Current RF Stability and Proposed Solution	4
	Appendix	7
A	Complementary Material Controller Design	7
B	Lab Test and Measurement Equipment	11
	Acknowledgments	15

List of Figures

1.1	Schematic of the FLUTE RF system	1
1.2	Plot of the electrical field in z direction over the length of the gun cavity (redrawn from [Bos+96] using geometrical measurements from [Hön14]) . .	2
1.3	Cross section drawing of the electron gun together with the solenoid (which is used for focusing the electron beam) showing the photo-cathode (red) and the electron and laser beam trajectories (modified version from [Bos+96] and [Bos+95])	3
1.4	Schematic of the FLUTE RF system with the proposed control unit and the controllable RF attenuator added	5
1.5	Deviation of the cavity RF power over the course of one hour	5
1.6	Periodogram of Figure 1.5; calculated using the Welch method	5
A.1	Screenshot of the Matlab System Identification Toolbox; to the right the process models estimator window	7
A.2	Screenshot of the Matlab PID Tuner from the Control Systems Toolbox . .	7
A.3	Simulink model to evaluate the designed controller together with the measurement filter (o11) compared to the uncontrolled system (in P2ZU) using measured disturbance data (in the vector d2); below a view of the scope data	8

List of Tables

B.1	Agilent 34411A specifications	11
B.2	Agilent 34411A some SCPI commands	11
B.3	Keysight 34470A specifications	11
B.4	Keysight 34470A some SCPI commands	11
B.5	Keysight 34972A specifications	11
B.6	Keysight 34972A some SCPI commands	12
B.7	Rohde and Schwarz SMC100A specifications	12
B.8	Rohde and Schwarz SMC100A some SCPI commands	12
B.9	HP E4419B specifications	12
B.10	HP E4419B some SCPI commands	12
B.11	Agilent E5071C specifications	13
B.12	Holzworth HA7062C specifications	13

Acronyms

BIBO Bounded Input Bounded Output. 7

CER Coherent Edge Radiation. 1

CSR Coherent Synchrotron Radiation. 1

CSS Control System Studio. 10

cSTART compact **S**torage ring for **A**ccelerator **R**esearch and **T**echnology. v, 1

DFT Discrete Fourier Transform. 4

ESD Energy Spectral Density. 4

FLUTE *F*erninfrarot *L*inac- und *T*est-*E*xperiment. v, 1, 3

KIT Karlsruhe Institute of Technology. v

LINAC Linear Accelerator. 1

LTI Linear Time Invariant. 7

PSD Power Spectral Density. 4, 5

RF Radio Frequency. v, 2

STFT Short Time Fourier Transform. 6

THz terahertz. v, 1

UV ultraviolet. 1, 2

WSS Wide Sense Stationary. 4

1. The Stability of FLUTE the Electron Gun and Proposed Stabilizing Solution

This chapter deals with the electron gun of FLUTE and its power supply. Then based on fundamental equations of electron gun's microwave cavity, the dependence of the electron energy from the RF supply is derived, which motivates why the RF supply should be stable. Then a solution to stabilize the RF is proposed.

The electron gun is powered by a 50 MW klystron, a high-power vacuum tube RF amplifier. The input signal for the klystron is a 2.998 55 GHz harmonic oscillator pre-amplified to 200 W. The supply input is generated by a pulse forming network and a transformer. The pulse forming network mainly consists of capacitors to store electrical energy and is charged with a constant current source. The connection of these devices is shown in Figure 1.1.

A 5 Hz master clock ("trigger") is used to switch on the output of the pulse forming network to the klystron and the oscillator every 0.2 s for 4.5 μ s. During this time, the laser could also be triggered causing a stimulated emission of an electron bunch from the cathode. But even without the laser being active, powering the electron gun with the klystron generates an electron beam through thermionic emission of electrons. This undesired effect is called *dark current*.

The current source to charge the pulse forming network is powered by mains voltage. This makes it susceptible to noise on the mains and also caused slowly time varying drifts of the klystron power due the pulse forming network being triggered at different relations to the mains 50 Hz. This issue has been remedied in [Nas+19] by adding synchronization to the mains phase.

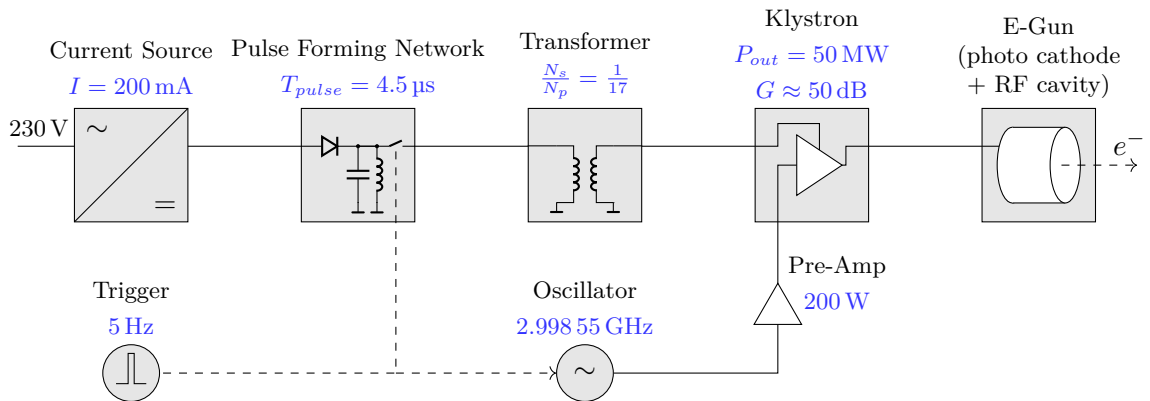


Figure 1.1: Schematic of the FLUTE RF system

1.1 The Electron Gun

The electron gun of FLUTE was originally designed and operated in CTF II at Conseil Européen pour la Recherche Nucléaire (CERN). [Sch+14] It is of the “BNL type” (see [Bat+88], based on the original design by [Fra+87]) and was developed at CERN. [Bos+95]

The gun is made up of a 2.5 cell microwave cavity with a removable copper cathode embedded in the cone shaped back at the end of the half cell (see Figure 1.3). Cooling is achieved with a two-stage water cooling system: A temperature control unit uses a short water circuit to cool the gun while itself uses a heat exchanger to a bigger outside climate unit.

Applying RF power to the cavity through the hole-coupled wave guide causes a standing wave inside the cavity. Because of the cavity’s dimensions, only the fundamental mode TM_{010} is excited, for which the relation between resonance frequency f_{010} and radius a of the cavity is given by

$$\frac{f_{010}}{2\pi} = \frac{2.405 \cdot c}{a}. \quad (1.1)$$

For the TM_{010} mode there is only an electrical field in the z direction, i.e. along the beam axis. This $E_z(z)$ field is used to accelerate the electrons. For the FLUTE gun, $E_z(z)$ has been measured in [Bos+96], see Figure 1.2. These measurements are also verified in [Sch+14].

To tune the resonance frequency f_{010} , which depends on the cavity’s radius a , to the target design frequency of 2.998 55 GHz, two methods are used. For once the cavity is equipped with piston tuners that allow changing the geometries of each cell slightly. Additionally because of the expansion and contraction of the copper body due to temperature changes, the set-point of the water cooling system can also be changed to alter the cavity geometry.

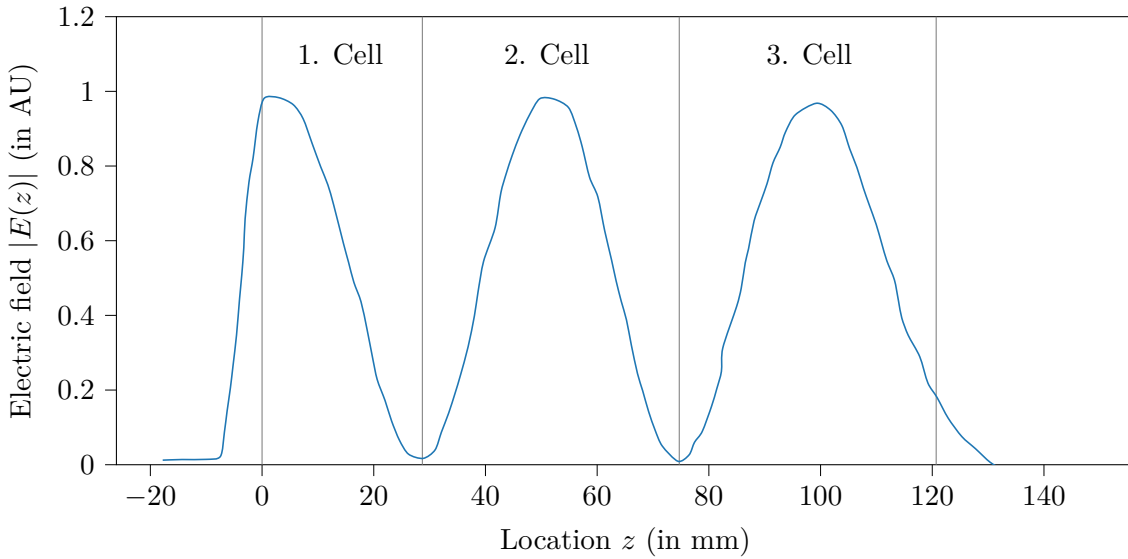


Figure 1.2: Plot of the electrical field in z direction over the length of the gun cavity (redrawn from [Bos+96] using geometrical measurements from [Hön14])

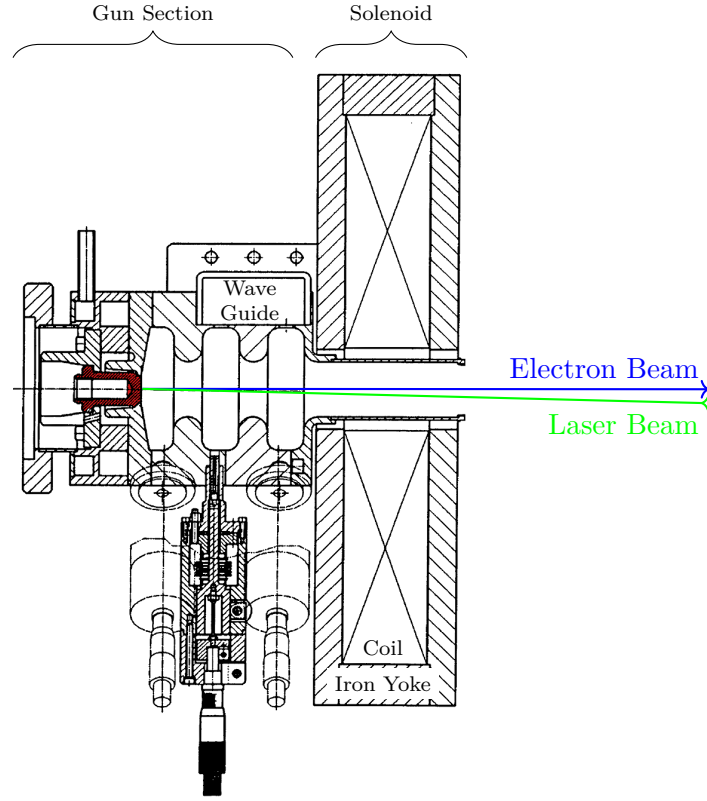


Figure 1.3: Cross section drawing of the electron gun together with the solenoid (which is used for focusing the electron beam) showing the photo-cathode (red) and the electron and laser beam trajectories (modified version from [Bos+96] and [Bos+95])

1.2 Relation between RF power and Electron Energy

A standing wave inside a RF cavity for a TM_{010} mode can be written as

$$E_z(z, t) = E(z) \cos(\omega t + \phi). \quad (1.2)$$

The time t has to be expressed in terms of the electron velocity $v(z)$ as

$$t = t(z) = \int_0^z \frac{dz}{v(z)}, \quad (1.3)$$

which is the arrival time of the electron at location z .

If moving through an accelerating gap of length L inside a cavity, an electron with charge q gains the energy

$$\Delta W = q \int_{-L/2}^{L/2} E(z) \cos(\omega t(z) + \phi) dz \quad (1.4)$$

This can be rewritten as

$$\Delta W = qV_0 T \cos(\phi) \quad (1.5)$$

using the axial RF voltage

$$V_o := \int_{-L/2}^{L/2} E(z) dz \quad (1.6)$$

and the travel time factor T . [Wan08, p. 32]

With the *shunt impedance* R_s , the axial RF voltage can be brought into relation with the RF power, that need to be induced into the cavity to compensate losses in the non-perfect conducting walls and power lost to the electron beam. [Bur]

The shunt impedance is defined as

$$R_s = \frac{V_0^2}{P_{\text{RF}}} \quad (1.7)$$

Equation 1.5 and Equation 1.7 show that the RF supply has a great impact on the electron energy, so it needs to be stable.

Additionally, there is the so called *R over Q*, defined as

$$\frac{R}{Q} = \frac{(V_0 T)^2}{\omega U} \quad \text{with: } R = R_s T^2 \text{ (effective shunt impedance)} \quad (1.8)$$

using the total stored electromagnetic energy U and the quality factor $Q = \omega U / P_{\text{RF}}$.

This shows the gained energy also depends on the properties of the cavity.

1.3 Current RF Stability and Proposed Solution

To get an overview of the current stability of the RF power, the deviation of the cavity power process value (Experimental Physics and Industrial Control System (EPICS): F:RF:LLRF:01:GunCav1:Power:Out Value) from its mean is plotted over one hour, see Figure 1.5.

With the metrics defined in ??, the %STD is 0.15 % and the MSE is 38.54.

From the time plot in Figure 1.5 and the periodogram in Figure 1.6 it becomes clear that there is random white noise, but also a periodic part and a slow drift in the signal. While it is not possible to counteract the random fluctuations by any practical means, it is however possible to compensate for the slower disturbances.

Hence in the next chapters, the control system is developed to counteract these noise components.

The control system should be made up with a controllable RF attenuator added to the existing RF system. This way there is no modification to the proprietary Low Level RF (LLRF)¹ necessary. With the addition of the control unit (see Figure 1.4), which is designed in later chapters and contains the controller $G(s)$ and the filter $H(s)$, the a closed-loop for feedback control is formed.

¹The LLRF is visualized as only the oscillator in Figure 1.1 and Figure 1.4 but contains also its own feedback system and a vector modulator

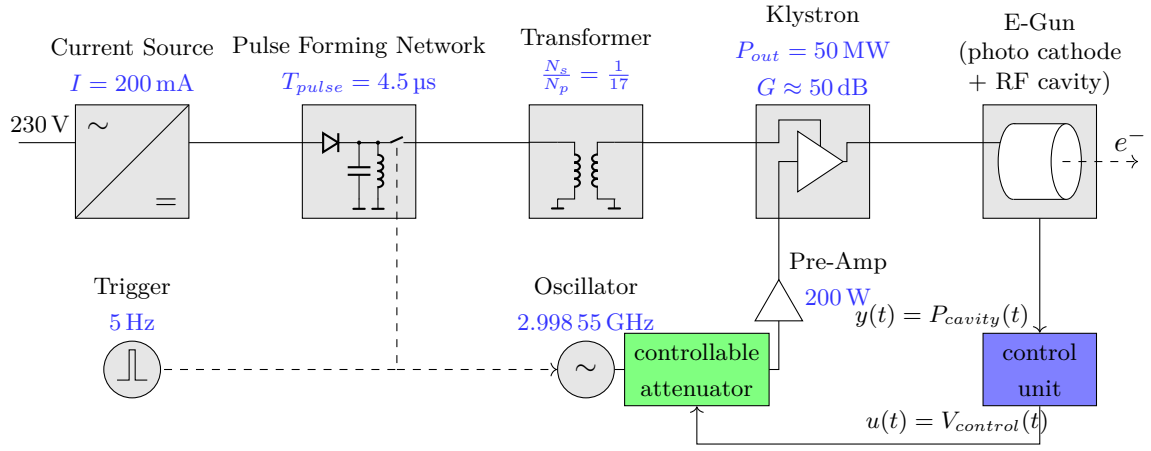


Figure 1.4: Schematic of the FLUTE RF system with the proposed control unit and the controllable RF attenuator added

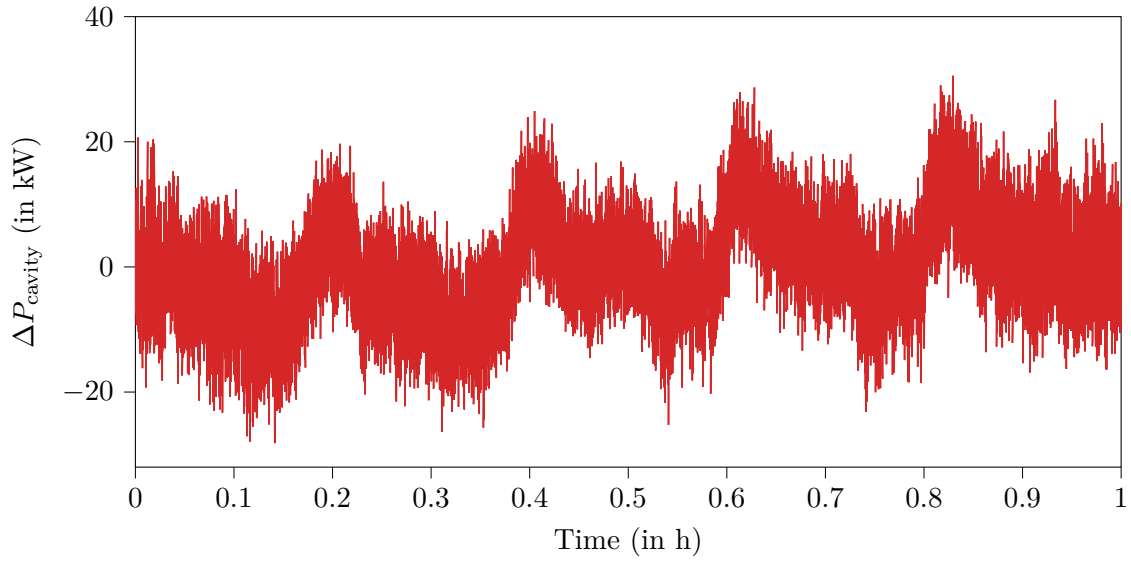


Figure 1.5: Deviation of the cavity RF power over the course of one hour

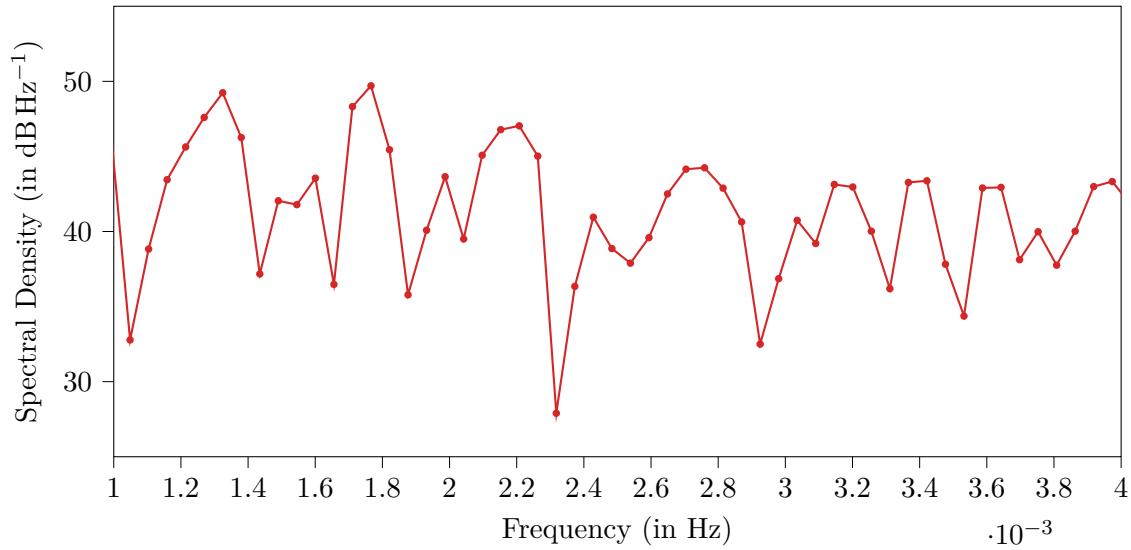


Figure 1.6: Periodogram of Figure 1.5; calculated using the Welch method

Appendix

A Complementary Material Controller Design

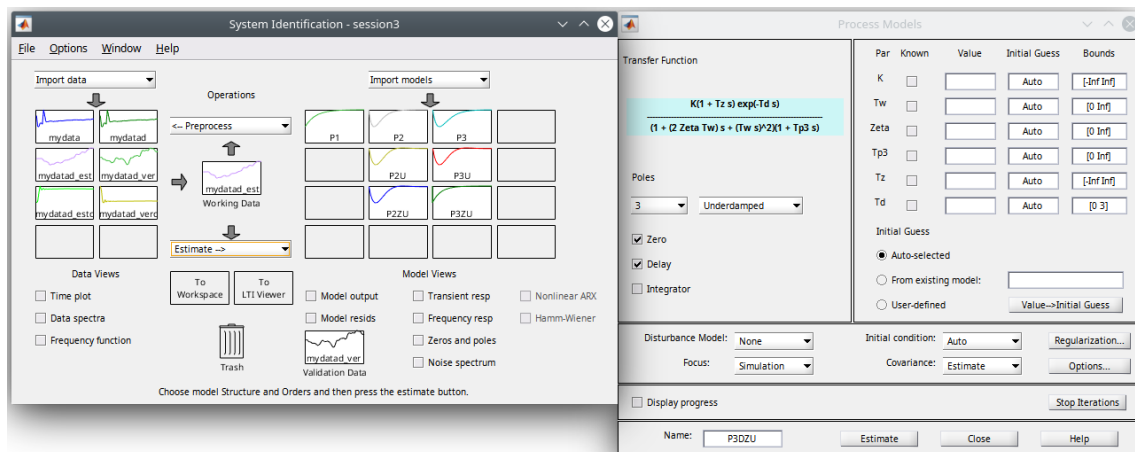


Figure A.1: Screenshot of the Matlab System Identification Toolbox; to the right the process models estimator window

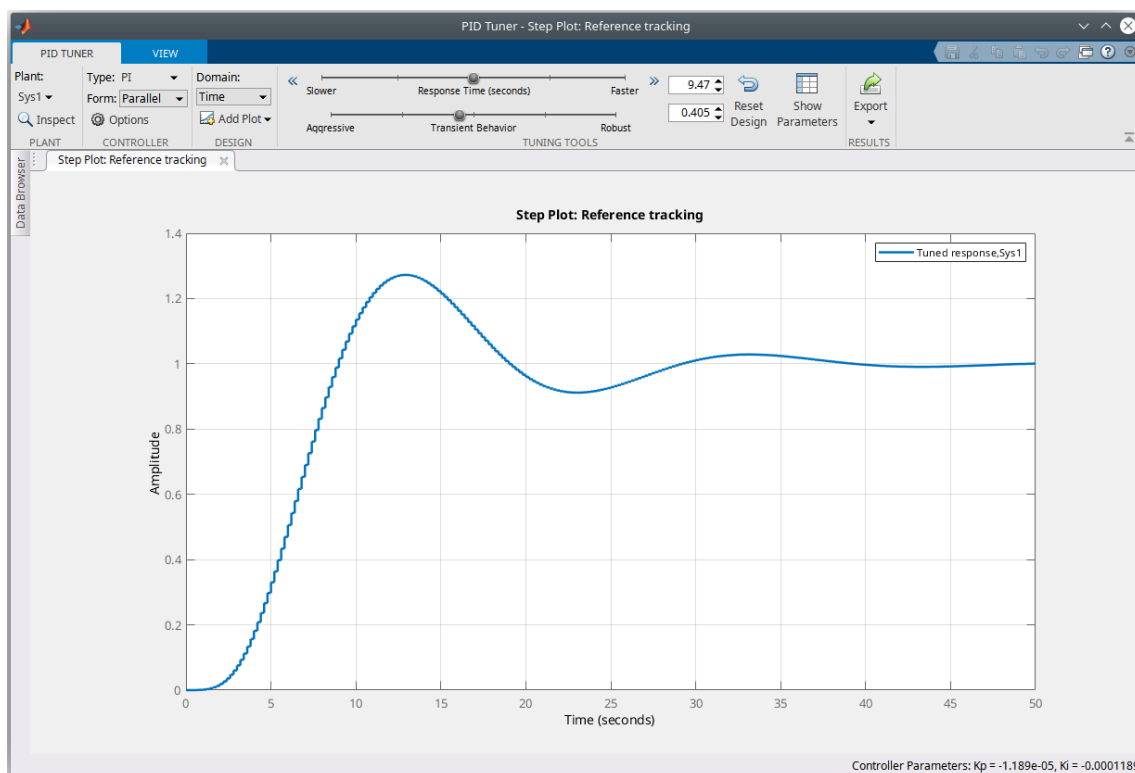


Figure A.2: Screenshot of the Matlab PID Tuner from the Control Systems Toolbox

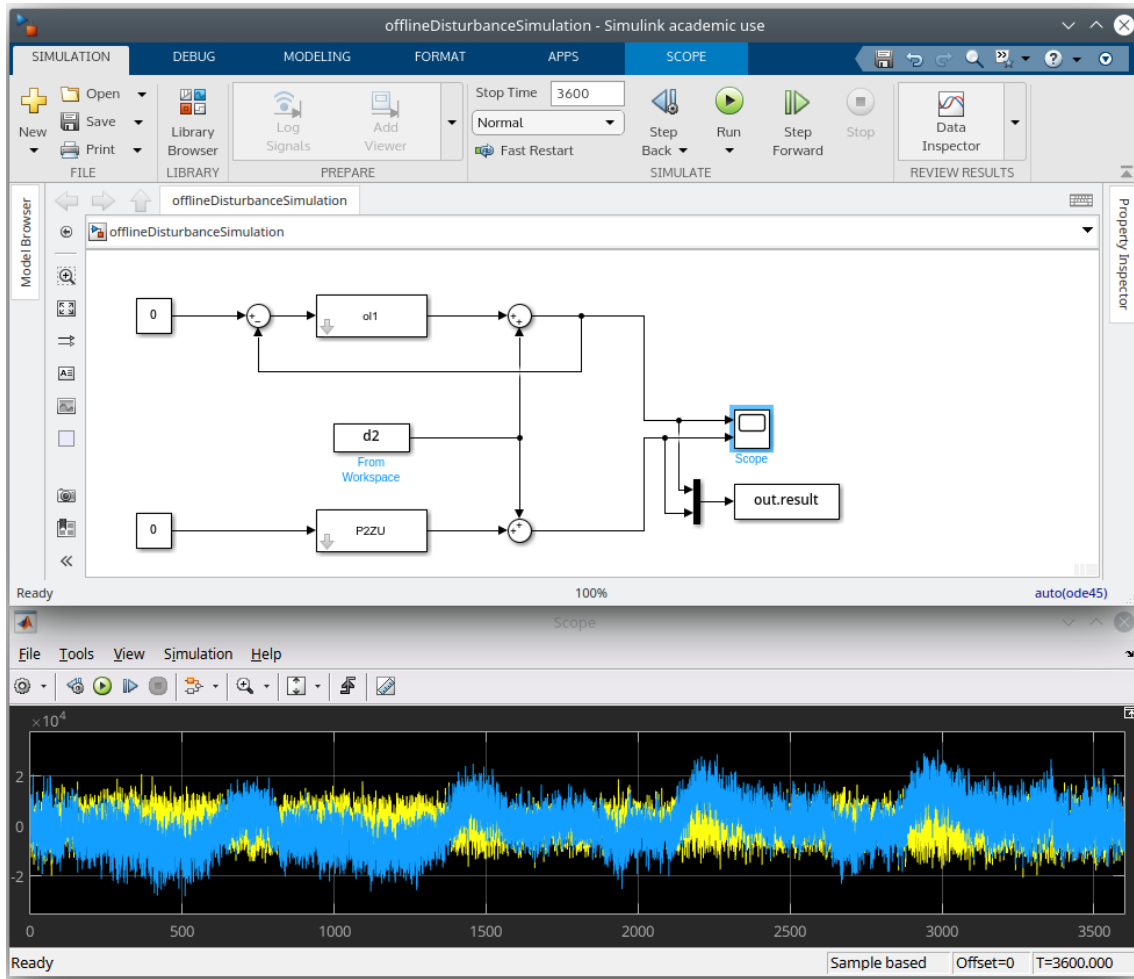


Figure A.3: Simulink model to evaluate the designed controller together with the measurement filter (ol1) compared to the uncontrolled system (in P2ZU) using measured disturbance data (in the vector d2); below a view of the scope data

Listing 1: Java class of the PCB421A25 charge amplifier demonstrating the command structure and checksum calculation for integration of the amplifier into Control System Studio (CSS)

```

1 class PCB421A25 {
2     final static char STX = '\u0002';
3     static enum FixedRange {
4         RANGE_1000000("01"),
5         RANGE_500000("02"),
6         RANGE_200000("03"),
7         RANGE_100000("04"),
8         RANGE_50000("05"),
9         RANGE_20000("06"),
10        RANGE_10000("07"),
11        RANGE_5000("08"),
12        RANGE_2000("09"),
13        RANGE_1000("10"),
14        RANGE_500("11"),
15        RANGE_200("12"),
16        RANGE_100("13");
17    public final String command;
18    private FixedRange(String command) {
19        this.command = command;
20    }
21 }

```

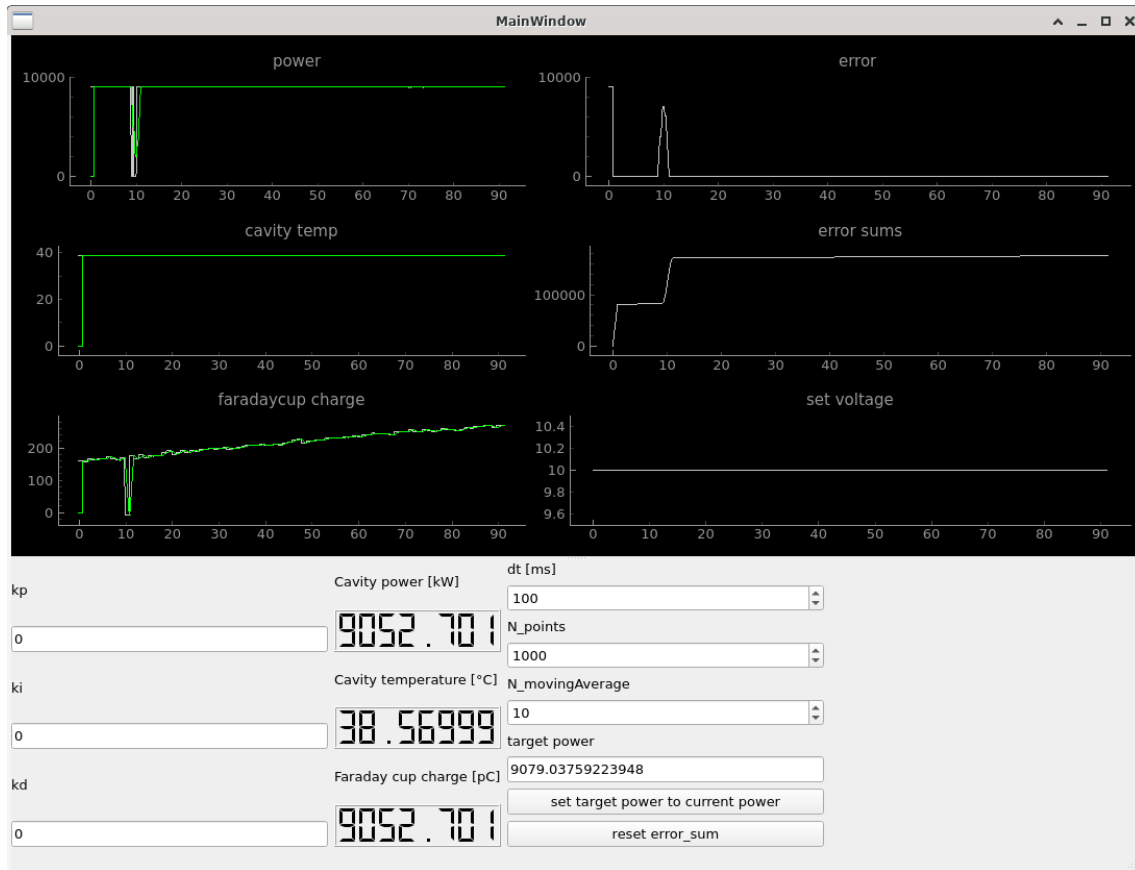


Figure A.4: Screenshot of the control system's GUI application

```

22
23 public PCB421A25() {};
24
25 public void setFixedRange(FixedRange fixedRange) {
26     String command=STX+"c"+"0"+fixedRange.command;
27     command += calculateChecksum(command);
28     sendCommand(command);
29 }
30
31 public boolean setVariableRange(int variableRange) {
32     if (!(variableRange>100 && variableRange<1000000)) return false;
33     String command=STX+"d"+"0"+String.format("%06d", variableRange);
34     command += calculateChecksum(command);
35     sendCommand(command);
36     return true;
37 }
38
39 private char calculateChecksum(String command) {
40     int checksum=0;
41     for(int i=0;i<command.length();i++)
42         checksum+=(int)command.charAt(i);
43     String checksum_hexstr=Integer.toHexString(checksum).toUpperCase();
44     return checksum_hexstr.charAt(checksum_hexstr.length()-1);
45 }
46
47 private void sendCommand(String command){
48     System.out.println("Command to send: "+command+" (length: "+command.length()+")");
49     // [...]
50 }
51

```

```
52 public static void main(String[] args) {  
53     PCB421A25 chargeSensitiveAmplifier = new PCB421A25();  
54  
55     //Test fixed ranges  
56     System.out.print("Fixed range 1000000;\t");  
57     chargeSensitiveAmplifier.setFixedRange(FixedRange.RANGE_1000000);  
58     System.out.print("Fixed range 100;\t");  
59     chargeSensitiveAmplifier.setFixedRange(FixedRange.RANGE_100);  
60  
61     //Test variable ranges  
62     System.out.print("Variable range 123456;\t");  
63     chargeSensitiveAmplifier.setVariableRange(23500);  
64     System.out.print("Variable range 999;\t");  
65     chargeSensitiveAmplifier.setVariableRange(999);  
66     }  
67 }
```

B Lab Test and Measurement Equipment

B.1 Benchtop multimeters

B.1.1 Agilent 34411A

Table B.1: Agilent 34411A specifications

Specification	Value
Digits	6 1/2
Measurement method	cont integrating multi-slope IV A/D converter
Accuracy (10 V range, 24 hours)	0.0015 % + 0.0004 % (% of reading + % of range)
Bandwidth	15 kHz (typ.)

Table B.2: Agilent 34411A some SCPI commands

Description	Example command	Example return
Read current measurement	READ?	+2.84829881E+00 (2.848 V)

B.1.2 Keysight 34470A

Table B.3: Keysight 34470A specifications

Specification	Value
Digits	7 1/2
Measurement method	cont integrating multi-slope IV A/D converter
Accuracy (10 V range, 24 hours)	0.0008 % + 0.0002 % (% of reading + % of range)
Bandwidth (10 V range)	15 kHz (typ.)

Table B.4: Keysight 34470A some SCPI commands

Description	Example command	Example return
Read current measurement	READ?	+9.99710196E+00 (9.997 V)

B.2 Data Acquisition/Switch Unit

B.2.1 Keysight 34972A

Table B.5: Keysight 34972A specifications

Specification	Value
34907A (Multifunction module)	
DAC range	± 12 V
DAC resolution	16 bit ($2^4 \text{ V} / 2^{16} = 366.21 \text{ } \mu\text{V}$ per bit)
DAC maximum current	10 mA
34901A (20 channel multiplexer)	

Table B.6: Keysight 34972A some SCPI commands

Description	Example command	Example return
Read current measurement	READ?	+2.00200000E+01 (20.02 °C)
Set DAC voltage of ch 204 to 3.1 V	SOUR:VOLT 3.1, (@204)	

B.3 RF signal generator

B.3.1 Rohde and Schwarz SMC100A

Table B.7: Rohde and Schwarz SMC100A specifications

Specification	Value
Frequency range	9 kHz to 3.2 GHz
Maximum power level	17 dBm
SSB phase noise (@ 1 GHz, $f_o = 20$ kHz, $BW = 1$ Hz)	-111 dBc
Level error	<0.9 dB

Table B.8: Rohde and Schwarz SMC100A some SCPI commands

Description	Example command	Example return
Set RF power level to 10.5 dBm	SOUR:POW 10.5	
Set RF frequency to 3.1 GHz	SOUR:FREQ:FIX 3.1e9	
Enable the RF output	OUTP on	

B.4 RF power meter

B.4.1 HP E4419B

Table B.9: HP E4419B specifications

Specification	Value
Digits	4
Accuracy (abs. without power sensor)	± 0.02 dB
Power probe: E4412A	
Frequency range	10 MHz to 18 GHz
Power range	-70 dBm to 20 dBm

Table B.10: HP E4419B some SCPI commands

Description	Example command	Example return
Measure power on input 1	MEAS1?	+2.89435802E+000 (2.894 dBm)

B.5 Vector Network Analyzer

B.5.1 Agilent E5071C

Table B.11: Agilent E5071C specifications

Specification	Value
Frequency range	9 kHz to 8.5 GHz

B.6 Phase noise analyzer

B.6.1 Holzworth HA7062C

Table B.12: Holzworth HA7062C specifications

Specification	Value
DUT input frequency	10 MHz to 6 GHz
Measurement bandwidth	0.1 Hz to 40 MHz offsets

Acknowledgments

First I would like to thank Prof. Anke-Susanne Müller and the whole FLUTE team for providing me with the opportunity to write my thesis at their research facility. FLUTE proved to be a one-of-a-kind machine and I really appreciate the work that has already been put into it.

I am very grateful to Prof. Dr.-Ing. John Jelonnek from the Institute for Pulsed Power and Microwave Technology for taking the responsibility of being my first reviewer. Also many thanks to his PhD students Benjamin Ell and Alexander Marek for listening patiently to my presentations and providing great support in optimizing them.

I'm especially in debt to my excellent advisor Dr. Nigel John Smale, for always having the time to go over both fundamentals and nifty details of electronics and physics alike. Without his support I wouldn't even be able to switch on FLUTE by now and much less a successful thesis would've been possible.

Valuable inputs from Andreas Böhm regarding the RF attenuator and electronics in general were a great help.

Thanks to Igor Križnar for constructive discussions and programming the graphical user interface and its back-end to control the charge sensitive amplifier.

Construction of the charge sensitive amplifiers connection box by Jürgen Schmid is greatly appreciated.

Thanks to Olena Manzhura from KIT-IPE for her support and for prove-reading the thesis multiple times.

Finally but maybe most importantly, a big thanks goes out to my family, that is my mom Sonja, Stefan and my grandparents Ernst and Gretel. I owe them my deepest appreciation for their support over the last years.

Bibliography

- [Bat+88] K. Batchelor et al. “Development of a high brightness electron gun for the Accelerator Test Facility at Brookhaven National Laboratory”. In: (Jan. 1988). URL: <https://www.osti.gov/biblio/7058521>.
- [Bos+95] Rudolf Bossart et al. “A 3 GHz photoelectron gun for high beam intensity”. In: (Sept. 1995). URL: <https://cds.cern.ch/record/288412>.
- [Bos+96] Rudolf Bossart et al. “CLIC-note 297 - A 3 GHz photoelectron gun for high beam intensity”. In: (1996).
- [Bur] G. Burt. *Introduction to RF for Accelerators*. Ed. by The Cockcroft Institute.
- [Fra+87] J. Fraser et al. “Photocathodes in accelerator applications”. In: Jan. 1987.
- [Hön14] Stephan Höninger. “Charakterisierung der Elektronenquelle für den Linearbeschleuniger FLUTE”. PhD thesis. Karlsruhe Institute of Technology - IBPT, 2014.
- [Nas+19] Michael Nasse et al. “First Electron Beam at the Linear Accelerator FLUTE at KIT”. en. In: *Proceedings of the 10th Int. Particle Accelerator Conf. IPAC2019* (2019), Australia. DOI: 10.18429/JACOW-IPAC2019-MOPTS018.
- [Sch+14] Marcel Schuh et al. “Status of FLUTE”. en. In: *Proceedings of the 5th Int. Particle Accelerator Conf. IPAC2014* (2014), Germany. DOI: 10.18429/JACOW-IPAC2014-MOPR0066.
- [Wan08] Thomas Wangler. *RF linear accelerators*. Weinheim: Wiley-VCH, 2008. ISBN: 9783527623426.